Available online at www.sciencedirect.com
ScienceDirect
Mendeleev Commun., 2006, **16(1)**, 11–13

Mendeleev Communications

Water permeation through MCM-41 channels: a molecular dynamics study

Kourosh Malek*[a,b] and Jihong Sun[a]

[a] *Key Laboratory of Energy and Chemical Engineering, Ningxia University, Yinchuan 750021, China*
[b] *Schuit Institute of Catalysis, ST/SKA, Eindhoven University of Technology, 5600 MB, Eindhoven, The Netherlands.*
E-mail: K.Malek@tue.nl

DOI: 10.1070/MC2006v016n01ABEH002217

Molecular dynamics simulations of water permeation through nanosized MCM-41 cylindrical channels showed a strong effect of channel size on water permeation and filling mechanism.

The permeation of water molecules in water-filled pores of nanometer dimensions is of interest in biology, chemistry and chemical engineering (*e.g.*, ion channels, mesoporous silica materials and carbon nanotubes).[1–3] The water–surface and water–water interactions can lead to a new structure of water in a nanopore, which is usually different from that in bulk water.[3] We studied the permeation and motion of water in cylindrical pores of the mesoporous silica material MCM-41 by means of molecular dynamics (MD) simulations. The pores of MCM-41 are roughly cylindrical with diameter ranging from 1.6 to 10 nm.[4,5] The dynamical properties of water molecules such as self-diffusion, hydrogen bonding and translational and rotational motions of water molecules in MCM-41 have been studied recently.[6–9] However, several issues remain unanswered such as the detailed atomistic nature of the permeation of water molecules in MCM-41 and the effect of pore size on water motion inside the pores. We wish to answer these questions by means of all-atom MD simulations.

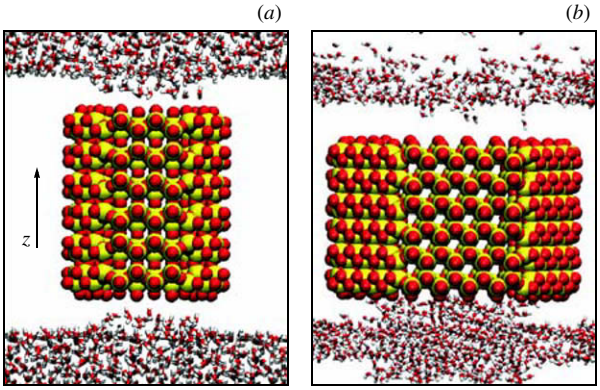

Figure 1 Side view of a part of the unit cells in systems *a* and *b*. The channel axis is along *z* and the front view is on the *xy* plane. MCM-41 channels are pictured as VDW. Water molecules in the reservoirs are pictured as licorice. Structures *a* and *b* are not drawn at the same scale.

In our MD simulations, MCM-41 channels are modelled based on straight three-dimensional channels (Figure 1). The structure is modelled by the pseudo cell Si_6O_{12}, which consists of hexagonal arrangements of Si–O–Si units. All silicon atoms at the pore surface are saturated by oxygen atoms. Oxygen atoms with fewer than two silicon atoms attached to them (at the inlet, outlet and outer surface), are then saturated by hydrogen atoms. Since the framework is not assumed to be rigid, the O and Si atoms are subject to move according to the equation of motion. At both ends, the pores open into reservoirs filled with single point charge (SPC) water. In the SPC model, the water molecule has fixed positive charges on the hydrogen atoms (+0.41) and an excessive negative charge on the oxygen atom (–0.82). To prevent the external part of the pore to become wet, a channel was fixed within a slab membrane opening to a bulk of water molecules in the two reservoirs at both ends. Simulations used the GROMOS96 force field.[10] In this force field, interactions between atoms are divided in non-bonded interactions between any pair of atoms that are within a given cut-off radius, and bonded interactions between atoms connected by chemical bonds. In case of non-bonded interactions (electrostatic and van der Waals), a partial charge and parameters for repulsion and attraction are assigned to each atom. The bonded interaction consists of bond, angle and dihedral terms. The Si–O bond stretching potential and O–Si–O bond angle bending are given by simple harmonic potentials, $V(R) = k_b(r_{Si-O} - r_{eq})/2$ and $V(\theta) = k_\theta(\theta - \theta_{eq})/2$, respectively, where $k_b = 2.5\times10^5$ kJ mol^{-1} nm^{-2} and $k_\theta = 0.17605$ kJ mol^{-1} deg^{-2}. The torsional rotational potential for the Si–O–Si–O dihedral angle is a periodic function with a three-fold barrier, $V(\phi) = = k_\phi[1 + \cos(3\phi)]/2$, where $k_\phi = -2.9289$ kJ mol^{-1}.[11] The hydrogen atoms attaching to oxygen were treated explicitly (as O–H). A cut-off of 1.4 nm was used for van der Waals interactions in our simulations. The integration time step was 2 fs. After that the systems were equilibrated for $\tau = 2$ ps using harmonic position restraints (1000 kJ mol^{-1} nm^{-2}), production runs were performed for another 1 ns under periodic boundary conditions and within an NVT ensemble. A Berendsen thermostat[10] with a time constant of 0.5 ps was used to maintain the temperature at 300 K. During the simulations, structures were saved every 500 steps (1 ps) and used for analysis.

Figure 1 shows instantaneous configurations of the MD systems, denoted as *a* and *b*. The channel in system *a* has an average Si–Si diameter of ~2.2 nm, while that in system *b* is ~ 4.2 nm. In both systems, the length of the channel is ~3.4 nm (Figures 1(*a*) and 1(*b*) are not at the same scale). Each system contains 4317 SPC water molecules with no water molecule inside the pore at $t = \tau$. The *z*-axial profile of the pore occupation of system *a*, *i.e.*, the total number of water molecules n_{water} along the channel as a function of time is shown in Figure 2(*a*). There are strong fluctuations in n_{water} inside the reservoirs. Overall, the profile is consistent with the filling procedure shown in Figure 2(*c*). There are remarkable moments within a complete permeation/filling procedure. The channel is empty at time $t = \tau$. The filling starts smoothly from the pore ends, forming two filled pore segments in the inlets. Further filling of the channels occurs as the filled pore segments growth. There is a filling threshold around $t = 6 + \tau$ ps, when the formation of an unbroken chain of water molecules in the middle of the pore causes a rapid filling of the channel. Such a 'percolating' chain has been already introduced as a possible water filling mechanism

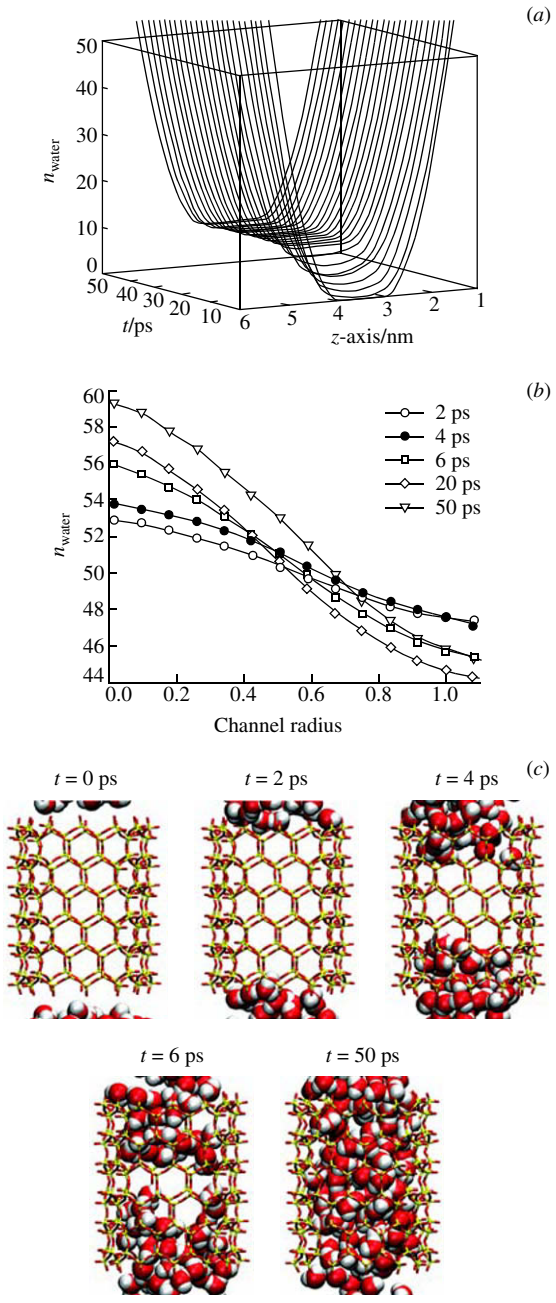

Figure 2 (*a*) Pore occupation profile of system *a* along the channel axis as a function of the pro-equilibrium time. (*b*) Radial occupation profile as a function of the pro-equilibrium time. (*c*) The filling process is shown by snapshots at the beginning $t = \tau$, $2 + \tau$, $4 + \tau$, $6 + \tau$ (filling threshold) and $50 + \tau$ ps.

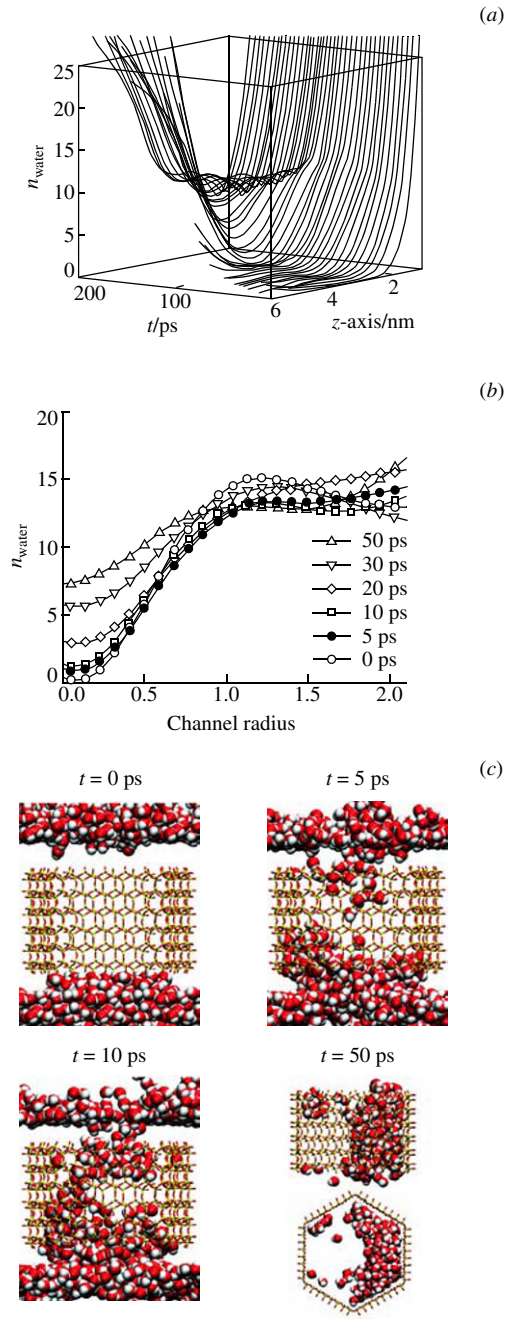

Figure 3 (*a*) Pore occupation profile of system *b* along the channel axis as a function of the pro-equilibrium time. (*b*) Radial occupation profile at different simulation times. (*c*) The filling process is shown by snapshots at different simulation times.

of a narrow carbon nanotube and the transition state in the filling process was analysed quantitatively.[12] In our MCM-41 channel, however, the chain of hydrogen-bonded water molecules only exists in the middle of the channel and is not spanning the whole channel, in contrast to the narrow carbon nanopore.[12] The channel filling proceeds around the percolating cluster and complete filling of the channel is achieved around $t = 50 + \tau$ ps. In the context of the permeation process, an important hint is the necessity of the initial wetting of the surface of the MCM-41 channels. The adsorption of water in MCM-41 (channel size of 3.3 nm) and SBA-15 (channel size of 8 nm) mesoporous silica materials was studied recently by ^{1}H magic angle spinning (MAS) and static solid state NMR spectroscopy.[7] This study leads to different pore-filling mechanisms for the two silica materials, and the initial wetting of the surface was suggested to occur in both channels. This may not be the case for a narrower MCM-41 channel. The radial profile of the channel occupation of system *a* is illustrated in Figure 2(*b*). There are more water molecules in the middle of the channel than in the vicinity of the channel wall. The number of water molecules inside the channel always fluctuates around 55, suggesting that the water molecules fill all the available radial volume. The latter shows no pre-wetting process for the MCM-41 channel of size 2.2 nm. We have also studied water permeation in a wider MCM-41 channel. Figures 3(*a*) and 3(*b*) show the *z*-axial and radial profiles of the channel occupation in system *b*, respectively. Figure 3(*a*) shows no evidence of forming water-filled pore segments in the inlets of a large MCM-41 channel of size 4.2 nm. Instead, after the permeation of water molecules and partial wetting of the surface, the filling occurs from the pore wall towards the centre of the pore [Figure 3(*c*)]. The latter is illustrated in the radial profile of the filling process as a function of time [Figure 3(*b*)]. These observations are in agreement with the experimental mechanism, suggested previously.[7] The motion of the water fluid in a confined channel can be better characterised by measuring the dynamic motion of water molecules, as well as water diffusivity

along the channel.[12–14] For example, a recent incoherent quasi-elastic neutron scattering (QENS) study of water confined in MCM-41 has shown a remarkable slowing down effect of confinement on both the translational and rotational relaxation times of water molecules.[6] Our preliminary analysis of the mean square displacement (MSD) for all water molecules in the MCM-41 channels did not show a diffusive motion within a time interval of 1 ns. This remarkable anomalous diffusion behaviour has been already observed experimentally[8] and is worthy of further computational investigation.[13,14]

The permeation of water molecules through two different MCM-41 mesopores with different pore diameters was studied by all-atom molecular dynamics simulations. The results show different filling mechanisms for the two channels. In a narrow channel (diameter of 2.2 nm), the filling occurs mainly in the direction of the pore axis. No initial wetting of the inner surface was observed for this channel. In a wider pore (diameter of 4.2 nm), the channel is filled radially after an initial partial-covering of the channel surface. The results are in good agreement with previous experimental data[7] and are important for the catalytic applications of mesoporous silica materials.

References

1 L. D. Gelb, K. E. Gubbins, R. Radhakrishan and M. Sliwinska-Batkowiak, *Rep. Prog. Phys*., 1999, **62**, 1573.
2 B. Smith, *J. Phys. Chem*., 1995, **99**, 5597.
3 G. Hummer, J. C. Rasaiah and J. P. Noworthya, *Nature*, 2001, **414**, 188.
4 B. Kuchta, P. Llewellyn, R. Denoyel and L. Firlej, *Coll. Surf. A*, 2004, **241**, 137.
5 K. Kleestorfer, H. Vinek and A. Jentys, *J. Mol. Catal. A*, 2001, **166**, 53.
6 A. Faraone, L. Liu, C.-Y. Mou, P.-C. Shih, J. R. D. Copley and S.-H. Chen, *J. Chem. Phys*., 2003, **119**, 3963.
7 B. Grünberg, T. Emmler, E. Gedat, I. Shenderonich, G. H. Findenegg, H.-H. Limbach and G. Buntkowsky, *Chem. Eur. J*., 2004, **10**, 5689.
8 F. Stallmach, J. Kärger, C. Krause, M. Jeschke and U. Oberhangemann, *J. Am. Chem. Soc*., 2000, **122**, 9237.
9 E. W. Hansen, R. Schmidt, M. Stöcker and D. Akporiaye, *Micropor. Mat*., 1995, **143**, 150.
10 W. F. van Gunsteren, P. Kruger, S. R. Billeter, A. E. Mark, A. A. Eising, W. R. P. Scott, P. H. Huneberger and I. G. Tironi, *The GROMOS96 Manual and User Guide*, Biomos and Hochschulverlag AG an der ETH Zürich, Groningen, 1996.
11 S. H. Lee and S. G. Choi, *Bull. Korean Chem. Soc*., 1999, **20**, 285.
12 R. Allen and J.-P. Hansen, *J. Chem. Phys*., 2003, **119**, 3905.
13 A. I. Skoulidas and D. S. Sholl, *J. Phys. Chem*., 2003, **107**, 10132.
14 K. Malek, T. Odijk and M.-O. Coppens, *Nanotechnology*, 2005, **16**, S522.

Received: 20th July 2005; Com. 05/2550